RSC Advances

RSC Advances

PAPER

Enhancement of Mechanical and Thermal Properties of Poplar through the Treatment of Glyoxal-Urea/Nano-SiO_2

Received 00th January 20xx,
Accepted 00th January 20xx

DOI: 10.1039/x0xx00000x
www.rsc.org/

Yutao Yan,[a] Youming Dong,[a] Jianzhang Li,[a,]* Shifeng Zhang,[a,]* Changlei Xia,[b] Sheldon Q. Shi[b] and Liping Cai[b]

Glyoxal is a cross-linking agent that could effectively improve dimensional stability and water resistance with compromising the mechanical properties of wood materials. This study explores relevant disadvantages of glyoxal-trated wood, and in effort to overcome the drawbacks, an environmental-friendly glyoxal-urea (GU) resin is synthesized from urea and glyoxal, and combined with nano-SiO_2 to treat Poplar wood. Results showed that the mechanical properties of the GU resin-treated wood were significantly increased compared to those of wood treated with glyoxal alone, and that incorporation of nano-SiO_2 in the GU resin further improved performance. The fracture morphology of GU/nano-SiO_2-treated wood was also characterized, indicating increased elasticity. Scanning electron microscope and energy dispersive X-ray (SEM-EDX) results showed that GU and nano-SiO_2 existed not only in the wood cell lumens, but also in the cell walls. Fourier transform infrared spectroscopy (FT-IR) test results showed the formation of GU resin and the incorporation of GU resin into the wood samples. Thermal analysis results demonstrated that thermal properties were improved after the incorporation of GU and nano-SiO_2 compared to samples solely glyoxal-treated. Improvement can most likely be attributed to increased cross-linkage length among the celluloses, and/or the filling effect of GU/SiO_2 in the voids in wood cell walls.

Introduction

Poplar (*Populus tomentosa* Carr.) is one of the most widespread, fast-growing, short rotation tree species in China. Because it grows so fast, Poplar is rather low in hardness and strength and shows inferior dimensional stability, which limits its general utilization. Modifying the wood to improve its physical and mechanical properties is an attractive endeavour, as its abundance would make its wider use very beneficial.

Glyoxal, a low volatile and non-toxic dialdehyde, is an effective cross-linking agent that is often used in the pulp and paper industry as a paper reinforcer, and in the textile industry as a fabric crease resistant finishing agent [1-6]. Due to its two active merged aldehyde groups, it can be used to glyoxylate the lignin in cell walls or cross-link with hydroxyl groups in cellulosic materials via a hemi-acetal or acetal reaction, in the presence of a catalyst [7-9]. In order to improve the dimensional stability of wood, previous researchers have used glyoxal as a cross-linking agent for wood modification [10-14]. All the modified wood in these studies exhibited excellent dimensional stability and reduced moisture absorption compared to the unmodified wood; however, the modification did not substantially improve the hardness of the wood. What's worse, the acidity of glyoxal and catalyst under high curing temperature may cause hydrolysis or degradation of cell walls [15, 16], thus reducing the mechanical properties of the wood and preventing its use as a load-bearing structural member.

Numerous studies have used formaldehyde-based thermosetting resins in attempt to improve mechanical properties and hardness of wood samples [17-22]. Though wood samples in these studies did show an improvement in mechanical properties after modification, formaldehyde-based materials posed significant environmental concerns. Owing to its low volatile and non-toxic, glyoxal-based synthetic resin is much more environmentally friendly. Urea (which, additionally, is favourably cost-effective) combines readily with glyoxal to form synthesized GU resin, improving wood samples' mechanical properties after application.

Nano-SiO_2 possesses several unique and advantageous properties including large specific surface area, high flame resistance, and high stability. It has been successfully applied in many fields, such as engineering materials, advanced materials, and polymer material industries (coating, rubber, adhesives, and plastics.) The incorporation of nanometre materials greatly improves the performance of any of these materials [23-30], however, nano-SiO_2 use remains relatively limited in the wood industry [31]. Shi (2007) used UF-nano-SiO_2 as a modification agent together with a coupling agent to treat Poplar wood in a previous study, where all treated wood samples showed improved hardness and mechanical properties [32]. Nano-SiO_2 was used in other studies, as well, to improve the mechanical, water uptake, dimensional stability,

---

[a] *MOE Key Laboratory of Wooden Material Science and Application; Beijing Key Laboratory of Wood Science and Engineering; MOE Engineering Research Centre of Forestry Biomass Materials and Bioenergy, Beijing Forestry University, Beijing 100083, China;.*
[b] *Department of Mechanical and Energy Engineering, University of North Texas, 3940 N Elm St., Suite F101, Denton, TX 76207, USA.*
** Corresponding authors: lijianzhang126@126.com; zhangshifeng2013@126.com.*

hardness, and flammability properties of wood-polymer composites (WPCs) [33-35]. Whether or not incorporation of nano-SiO_2 has a similarly positive effect on GU resin-modified wood remains unclear, however, especially as far as mechanical and thermal properties.

In this study, low acidic and environmental-friendly GU resin was synthesized from glyoxal and urea, combined with nano-SiO_2, and applied to Poplar wood samples. The primary objective of this study is to detail the effects of GU resin and nano-SiO_2 impregnation on the mechanical and thermal properties of Poplar.

Results and discussion

Physical and mechanical properties

Physical properties of GU/SiO_2-modified wood

Table 1 Physical properties of GU/SiO_2 modified wood

Sample particulars	ASE (%)	WPG (%)	Leachability (%)	24-h WU (%)
Untreated	——	——	——	108.17 ± 4.51
Glyoxal	68.70 ± 3.70	37.19 ± 2.19	16.23 ± 0.75	45.13 ± 3.11
GU	52.29 ± 2.52	56.05 ± 4.74	65.98 ± 3.64	72.22 ± 3.34
GU + 0.2% SiO_2	46.29 ± 5.39	50.11 ± 5.33	66.46 ± 1.95	59.77 ± 3.58
GU + 0.5% SiO_2	50.23 ± 2.26	57.59 ± 6.53	65.53 ± 1.10	57.39 ± 5.09
GU + 0.8% SiO_2	47.04 ± 3.97	52.24 ± 5.59	64.96 ± 3.09	68.29 ± 5.78
GU + 1.1% SiO_2	50.11 ± 2.75	54.62 ± 5.78	63.57 ± 3.47	63.57 ± 3.47

Note: GU = glyoxal urea resin; ASE = anti-swelling efficiency; WPG = weight percentage gain; WU = water uptake. SiO_2 addition is defined based on the weight percentage of the entire modifying agent.

Table 1 shows the physical properties of treated and untreated wood samples. Glyoxal is very effective in wood modification, able to endow wood with high dimensional stability (ASE up to 68.7%), low water uptake (45.3%) and low leachability (16.2%), as likewise demonstrated in previous research [14, 36]. After the GU resin synthesized from glyoxal and urea was introduced to the wood, dimensional stability and water resistance decreased in the samples compared to those modified by glyoxal alone especially the anti leachability. These results were likely caused by the poor water resistance of GU resin, which has a large amount of hydrophilic hydroxyl groups. In addition, the remaining unreacted urea and catalyst in treated wood could also lead to the high leachability. As shown in Table 1, the amount of nano-SiO_2 added to the GU resin does not evidently affect dimensional stability, weight percentage gain, or leachability of the wood samples, aside from a slight decrease in WU likely caused by nano-SiO_2 filling voids in the cell walls. To this effect, neither urea nor nano-SiO_2 contributed significantly to improvement of the physical properties of glyoxal-modified wood. Though the modified wood had a decreased water resistance ability compared to the glyoxal-treated wood, it was suitable to be used as an indoor material in flooring and furniture.

Mechanical properties of GU/SiO_2 modified wood

Table 2 Mechanical properties of GU/SiO_2 modified wood

Sample Particulars	MOR (MPa)	MOE (MPa)	CS (MPa)	Hardness (Shore D)
Untreated	72.75 ± 5.55	4355.83 ± 294.56	46.06 ± 2.24	46.35 ± 3.26
Glyoxal	38.32 ± 2.87	5373.83 ± 134.74	54.94 ± 4.94	53.77 ± 2.57
GU	51.14 ± 1.57	5909.83 ± 325.68	55.25 ± 3.97	57.32 ± 4.04
GU + 0.2% SiO_2	54.53 ± 6.33	6057.33 ± 743.34	61.08 ± 4.73	62.11 ± 3.39
GU + 0.5% SiO_2	64.08 ± 4.08	7069.00 ± 453.16	65.55 ± 3.07	61.55 ± 3.88
GU + 0.8% SiO_2	62.63 ± 3.19	6948.33 ± 317.01	64.59 ± 3.62	62.27 ± 2.09
GU + 1.1% SiO_2	62.58 ± 6.40	6938.33 ± 450.51	64.09 ± 3.90	61.33 ± 2.67

Note: GU = glyoxal urea resin; MOR = modulus of rupture; MOE = modulus of elasticity; CS = compression strength parallel to grain and hardness. SiO_2 addition is defined by weight percentage of the entire modifying agent.

Glyoxal treatment affected wood samples' MOR the most. As shown in Table 2, after glyoxal modification, the MOR of wood decreased by 47.3% while other mechanical properties improved. The reduction in MOR may be caused by hydrolysis or degradation of wood cell wall components under high acidity conditions and high temperatures during the curing process [15, 37]. In addition, short cross-linkage formed by glyoxal during the cross-linking reaction considerably restrained the relative mobility of cellulose molecules chain when suffering an external force, likely resulting in the stress concentration of the fibre network and increasing the brittleness of the wood [2]. After GU resin was applied, the wood's mechanical properties were improved over those modified solely by glyoxal. Enhanced properties can likely be attributed to reduced acidity and increased cross-linkage length after the incorporation of GU resin.

Once nano-SiO_2 was introduced to the GU resin, all the mechanical properties of modified wood were even further improved. As shown in Table 2, when 0.5% nano-SiO_2 was added, MOR increased by about 25.3%, MOE by 19.6%, and CS by 18.6% compared to those modified by GU. Hardness also slightly increased (by 7.4%). Improvement in mechanical properties may be attributable to the three-dimensional network structure of nano-SiO_2 [32] and its small size nano-effect (Nano-SiO_2 was ultrafine particle. Because of its large surface-to-volume ratio, the arrangement of atoms at the interface is quite chaotic. When suffering an external force they are easy to be deformed and migrated. Thus the nano-SiO_2 could efficiently transfer the stress across the composite components and endow the material with good toughness and ductility)[38]. After the nano-SiO_2 was dispersed in the GU resin and impregnated into the wood under pressure, it remained in the GU resin or deposited inside voids in the wood cell walls, increasing the wood's hardness and allowing better load transfer. At nano-SiO_2 addition over 0.5%, the mechanical properties did not significantly improve any further.

Morphology analysis

Fracture morphology analysis

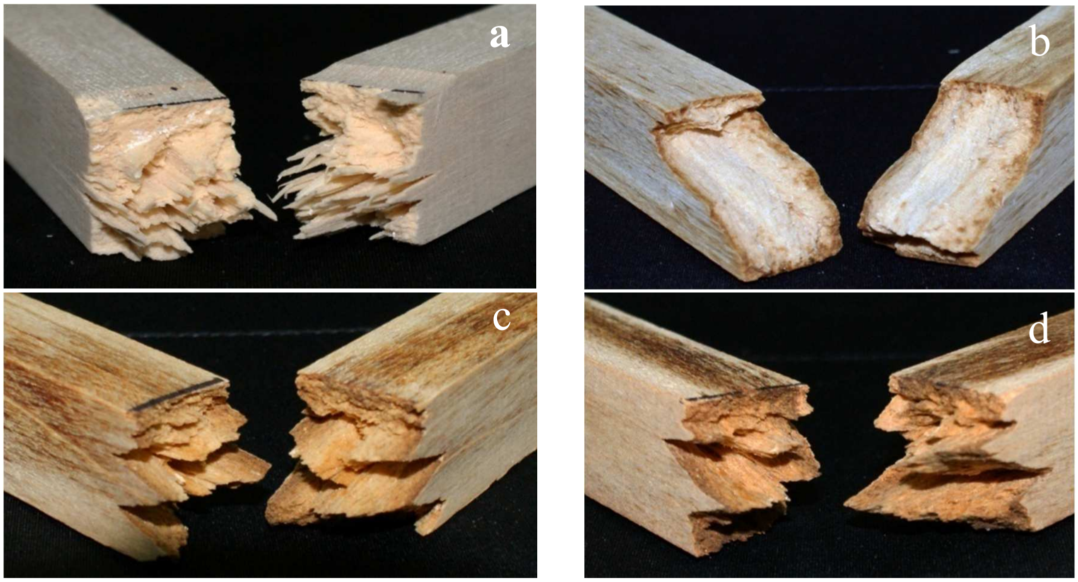

Fig. 1 Bending fracture morphology, a: untreated wood; b: treated by glyoxal; c: treated by GU resin; d: treated by GU with nano-SiO_2.

Fig. 1 shows the fracture morphology of treated and untreated wood on broken bending specimens. Untreated wood showed irregular fracture surface with jagged breakage line (Fig. 1a), similar to the research results shown by Xie [37]. Glyoxal-treated wood showed a smooth fracture surface (Fig. 1b), likely caused by brittle breakage under the high cross-linking density and short cross-linkage formed between the glyoxal and wood that increased brittleness. For specimens treated by GU resin, fracture surface showed large, jagged breakages with some smooth surfaces (Fig. 1c), indicating a decrease in brittleness. When nano-SiO_2 was added, the fracture morphology (Fig. 1d) did not change very much. Basically, glyoxal treatment made the wood much more brittle and prone to breakage, preventing its use as load-bearing structural member. The incorporation of urea and nano-SiO_2 improved the elasticity of the wood specimens, suggesting that it could be applied to load-bearing structures after modification.

SEM-EDX analysis

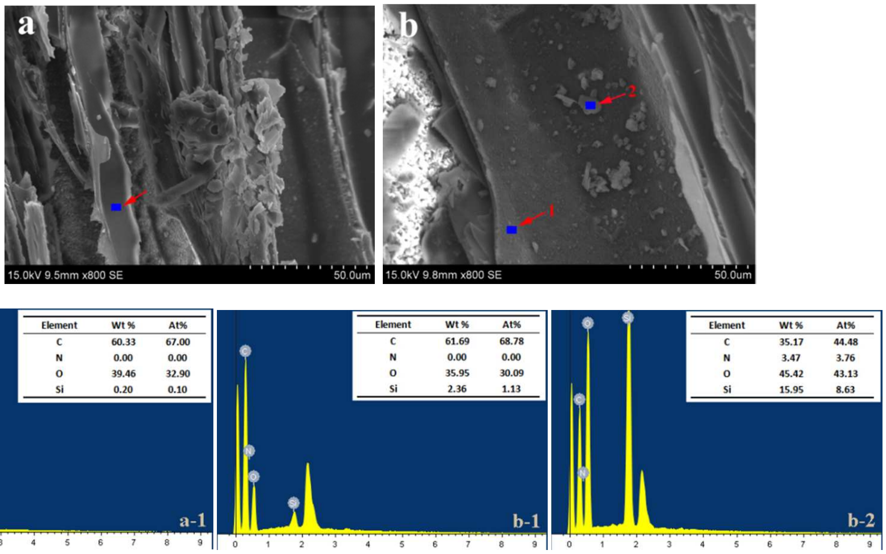

Element	Wt %	At%
C	60.33	67.00
N	0.00	0.00
O	39.46	32.90
Si	0.20	0.10

Element	Wt %	At%
C	61.69	68.78
N	0.00	0.00
O	35.95	30.09
Si	2.36	1.13

Element	Wt %	At%
C	35.17	44.48
N	3.47	3.76
O	45.42	43.13
Si	15.95	8.63

Fig. 2 SEM-EDX of GU-treated wood, a: without nano-SiO_2; b: with nano-SiO_2.

SEM analyses of GU-treated wood specimens without or with nano-SiO_2 are shown in Fig. 2a and b, respectively. As shown in Fig. 2a, wax-like substances formed on the wood cell walls, caused by impregnation of the GU resin. In Fig. 2b, numerous granular substances are visible on the surfaces of wood cell lumens, due to the aggregation of nano-SiO_2. EDX mapping was used to further demonstrate whether the nano-SiO_2 was incorporated into the wood cell walls. Fig. 2a-1 shows the element composition of a small area on the cell wall, marked by red arrows. Results suggest that almost no Si was present on the cell walls of the GU-modified wood. Based on SEM-EDX results, silicon content was about 0.2%; however, nano-SiO_2 was 2.4% (Fig. 2b-1) in the GU/nano-SiO_2-treated wood, and 16.0% (Fig. 2b-2) at the aggregation area in the cell lumens. Nano-SiO_2 was not only successfully introduced into the wood cell lumens, but also into the cell walls, thus influencing the mechanical properties of the modified wood. However, because of the limited resolving ability of EDX and the overlapping effect of high content of C element on N element, the determined N content in both Fig. 2 a-1 and Fig. 2 b-1 were zero.

FT-IR analysis

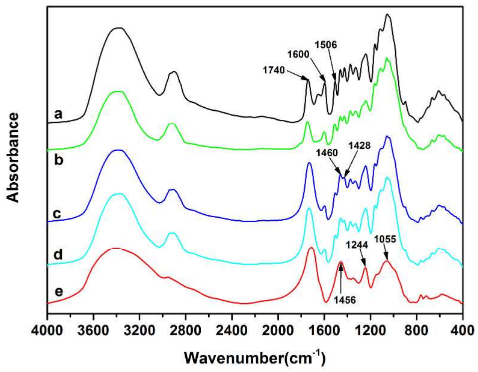

Fig. 3 IR spectroscopy of different specimens, a: untreated; b: glyoxal-treated; c: GU-treated; d: GU + 0.5 % nano-SiO_2-treated; e: pure cured GU resin.

Before impregnation, synthetic GU resin was cured and characterized by FT- IR. As shown in Fig. 3e, the broad and round band that occurs around 3,400 cm^{-1} was attributed to superposition of N-H in the amino groups and O-H stretching vibration in the hydroxyl groups. The absorption position and intensity of these peaks was multi-hydroxyl in the UG resin [39]. At the peak around 1,710 cm^{-1} there was a distinct characteristic absorption peak that was caused by the carbonyl group (-C=O) in the amide group. Symmetric stretching vibrations of carbon-oxygen (-C-O) bonds caused the absorption band at 1456 cm^{-1}. The other two absorption peaks at 1244 cm^{-1} and 1055 cm^{-1} were attributed to the coupling of carbon-nitrogen (-C-N) bond stretching vibration and nitrogen-hydrogen (-NH) bond bending stretching [40]. Based on these results, the reaction mechanism during the synthesis of GU resin can be described as shown in Fig. 4b.

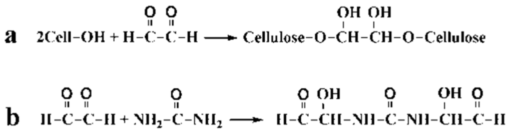

$$\mathbf{a}\quad 2\text{Cell-OH} + \text{H-}\overset{\text{O}}{\text{C}}\text{-}\overset{\text{O}}{\text{C}}\text{-H} \longrightarrow \text{Cellulose-O-}\overset{\text{OH}}{\text{CH}}\text{-}\overset{\text{OH}}{\text{CH}}\text{-O-Cellulose}$$

$$\mathbf{b}\quad \text{H-}\overset{\text{O}}{\text{C}}\text{-}\overset{\text{O}}{\text{C}}\text{-H} + \text{NH}_2\text{-}\overset{\text{O}}{\text{C}}\text{-NH}_2 \longrightarrow \text{H-}\overset{\text{O}}{\text{C}}\text{-}\overset{\text{OH}}{\text{CH}}\text{-NH-}\overset{\text{O}}{\text{C}}\text{-NH-}\overset{\text{OH}}{\text{CH}}\text{-}\overset{\text{O}}{\text{C}}\text{-H}$$

Fig. 4 Reaction mechanism, a: glyoxal with wood cellulose; b: glyoxal with urea.

The FT-IR spectra of treated and untreated specimens are shown in Fig. 3a-d. The absorbance around 1, 510 cm^{-1} was the characteristic absorption peak of benzene ring stretching vibration in lignin [41-43], which remained stable throughout treatment and thus provides a benchmark. The peak around 1,740 cm^{-1} assigned to carbonyl groups (-C=O) increased after GU resin treatment compared to untreated and glyoxal-treated specimens, suggesting that more carbonyl groups (-C=O) formed (Fig. 4b) [36] and that GU resin was effectively incorporated into the wood. The two absorption peaks at 1244 cm^{-1} and 1055 cm^{-1} ascribed to -C-N stretching vibration and -NH bending stretching also appeared in Fig. 3c and Fig. 3d. The band at 1460 cm^{-1} caused by stretching vibration of the carbon-nitrogen (-C-N) bonds [40] increased significantly. These results altogether confirmed the successful incorporation of GU resin into the wood samples. The absorption at 1,160 cm^{-1} due to antisymmetric bridge stretching vibration (C-O-C) increased in the glyoxal-treated wood, revealing the formation of ester bonds during treatment (Fig. 4a) [11, 13, 41, 42]. Absorption decreased in the GU resin-treated wood, however, possibly indicating that GU did not react with the wood. Whether or not GU resin reacts with wood components yet requires further investigation.

Thermal properties

TG and LOI analysis

Table 3 Degradation temperature and limiting oxygen index (LOI) of treated and untreated specimens.

Specimens	T_i	T_m	T_f	Temperature of decomposition (T_d) in K at different mass loss (%)				RW% at 600°C	LOI/%
				20%	40%	60%	80%		
Untreated	306.06	362.44	382.58	298.56	336.00	358.57	379.71	11.76	24.0 ± 0.3
Glyoxal treated	171.54	295.97	351.79	242.31	292.88	332.73	525.51	18.44	26.0 ± 0.1
GU without SiO_2	249.56	303.05	352.90	258.84	301.44	347.10	——	21.18	26.5 ± 0.2
GU with 0.2% SiO_2	249.11	305.30	358.99	264.41	308.03	343.93	——	21.55	27.0 ± 0.4
GU with 0.5% SiO_2	254.86	313.40	362.04	270.74	309.20	345.67	——	21.85	28.0 ± 0.2
GU with 0.8% SiO_2	253.13	308.95	358.90	267.87	307.97	351.99	——	22.32	29.0 ± 0.1
GU with 1.1% SiO_2	255.58	311.96	357.84	267.30	307.50	345.63	——	21.54	29.5 ± 0.3

Note: GU = glyoxal urea resin. All SiO_2 addition is defined by weight percentage of the entire modifying agent.

Table 3 shows initial decomposition temperatures (T_i), maximum degradation temperatures (T_m), final degradation temperatures (T_f), and residual weights (RW) of the untreated and GU/nano-SiO_2-treated wood specimens. The T_i, Tm, and T_f of specimens all greatly decreased after glyoxal treatment, indicating that glyoxal reduces the thermal stability of modified wood. This may be attributable to the degradation or hydrolysis of wood cell walls under the high curing temperatures in the presence of acidic glyoxal solution and acidic catalyst $(NH_4)_2S_2O_8$. When GU resin was applied, the degradation temperatures of all specimens increased, though they remained lower than those of the untreated specimens. This increase was likely caused by both the reduced acidity and increased chain length of the GU resin compared to pure glyoxal. Increased RW was probably also caused by increased chain length. When nano-SiO_2 was incorporated, the degradation temperatures of all specimens again further increased, but not significantly. The optimal nano-SiO_2 amount was determined at 0.5%, as the highest decomposition temperature was obtained at this percentage level for all specimens. The amount of nano-SiO_2 used (up to 1.1%) did not change the amount of residue, however.

Flame resistance properties of the wood specimens were examined by measuring their limiting oxygen index (LOI). As shown in Table 3, LOI gradually increased after GU and nano-SiO_2 were incorporated, indicating improved thermal stability and fire resistance.

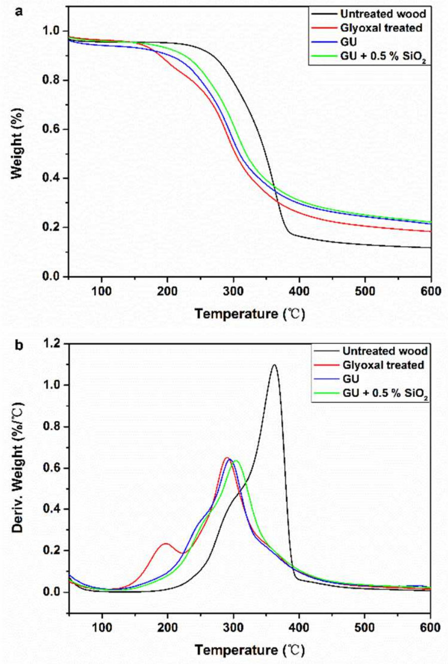

Fig. 5 TG curves of treated and untreated wood, a: TGA curves; b: DTG curves.

TGA and derivative thermogravimetry (DTG) curves of different wood specimens are presented in Fig. 5. Three distinct stages exist in the TGA curves. Stage I (room temperature to about 120°C) was a dehydration process, in which free water in the specimens evaporated. Mass loss during this period ranged from 3% to 4.5%. Stage II (120°C to 360°C) was where the most mass loss (around 60%) occurred, mainly caused by the thermal degradation of hemi-cellulose and cellulose that decomposed into char residues and CO_2, CO, CH_4, CH_3OH, and CH_3COOH. In this range, the mass loss rate of treated specimens was faster than that of untreated wood, indicating that the thermal stability of the wood had reduced. Fig. 5b also shows that the maximum rate of mass loss of treated wood (around 310°C) was smaller than that of untreated wood (around 360°C). Although all treated wood samples showed lower stability than the untreated sample, the stability of GU and GU-SiO_2-treated specimens was higher than those treated with only glyoxal, suggesting that the incorporation of urea and nano-SiO_2 improved the thermal stability of the wood. An additional 30% mass loss happened during Stage III (after 360°C), primarily due to the degradation of lignin [44].

DMA analysis

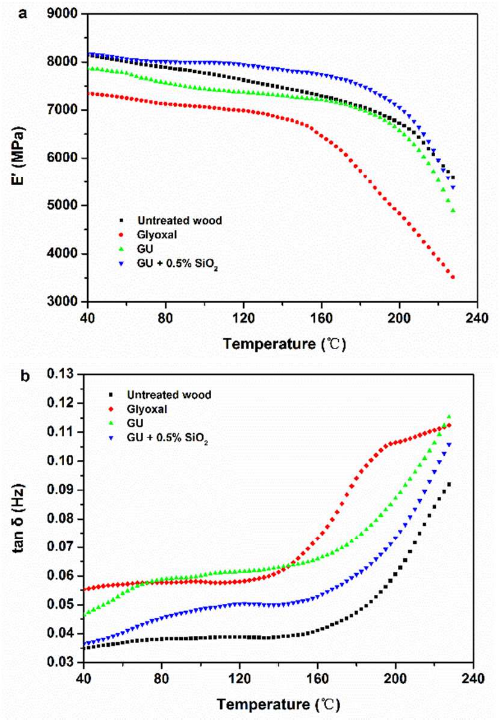

Fig. 6 DMA curves of treated and untreated wood, a: storage modulus; b: loss tangent.

Storage modulus is a crucial index for measuring the energy storage capability of material after elastic deformation, which was an index of resilience. Fig. 6a shows the storage modulus E’ of treated and untreated wood specimens. Storage modulus decreased as temperature increased, attributed to increased chain mobility of the polymeric components of the wood cell walls at higher temperatures [45]. Similar to the MOR property, after glyoxal treatment, storage modulus E’ decreased considerably compared to the untreated sample. The decrease in E’ demonstrates that glyoxal treatment reduced the elastic properties of the wood samples and increased their brittleness, probably caused by short cross-linkage between the celluloses and acidic hydrolysis or degradation of cell walls under high acidity and high temperature. (These effects also explain the brittle fracture shown in Fig. 1b.) When only GU resin was used to modify the wood, storage modulus was higher than in the glyoxal-treated sample, where cross-linkage length between wood celluloses increased. As a result, stress was more easily transferred [46] and macro mechanical properties improved. Storage modulus further increased when nano-SiO_2 was incorporated into the wood, where the three-dimensional network structure of nano-SiO_2 increased the strength of the wood and helped to transfer stress.

Wood possesses both viscose and elastic properties [47]. When a wood sample deforms, some energy is stored as potential energy, and some is dissipated as heat energy [48]. Fig. 6b shows the loss tangent (tan δ) of treated and untreated wood specimens, reflecting the damping of molecular movement within the material. The greater the tan δ, the harder the flow of the viscous molecules, and the greater the energy dissipated. When the wood was treated by glyoxal, many short cross-links formed between the cellulose polymer chains, restricting the movement of the chains and thus increasing the damping effect. When GU and nano-SiO_2 were incorporated, the tan δ decreased due to increased cross-linkage length among the cellulose polymer chains. This made the material more flexible and reduced the damping effect. The interfacial interaction between nano-SiO_2 and GU resin also limited the motion of resin molecules and helped to transfer some energy, reducing energy dissipation [49].

Conclusions

This study successfully synthesized and applied environment-friendly GU resin to modify Poplar wood. Experiment and analysis results show that the mechanical properties of GU resin-treated wood significantly improved over wood treated with solely glyoxal, primarily caused by the reduced acidity of GU resin after the copolymerization between urea and glyoxal which increased the length of cross-linked bonds in the crosslinking network, increasing elasticity and reducing degradation in the wood cell walls. When nano-SiO_2 was additionally introduced into the GU resin, all mechanical properties of the modified wood samples improved further, facilitated by the unique three-dimensional network, favourable properties (flame resistance and high stability,) and physical crosslinking between the nano-SiO_2 and UG resin. TG analysis showed that though all treated wood samples had lower stability than the untreated sample, the stability of GU and GU-SiO_2-treated wood was higher than other samples. DMA characterization further proved the beneficial effects of GU resin and nano-SiO_2 incorporation on the thermodynamics of the modified wood. SEM-EDX analysis indicated that nano-SiO_2 was present not only in the wood cell lumens, but also in the cell walls. In conclusion, after modification, the wood is suitable for indoor material application (flooring and furniture).

Experimental

Chemicals

Laboratory-grade glyoxal was obtained in 40% aqueous solution. Ammonium persulfate [$(NH_4)_2S_2O_8$] was analytical reagent grade. Solid urea (CON_2H_4) was industrial reagent. All chemicals used were provided by the Lanyi Chemical Reagent Company, China. Nano-SiO_2 with particle size of 15 ± 5 nm was supplied by Shanghai Maikun Chemical Co., Ltd., China.

Synthesis of glyoxal-urea resin

Appropriate amounts of urea and distilled water were added to a three-necked flask, stirred, and heated to 40°C. According to a specific mole ratio of 2 to 1 (based on the urea), glyoxal was added to the urea once completely dissolved. The pH value of the solution was adjusted to 4.0-5.0, and 1 wt% (based on the total weight of the solution) ammonium persulfate was added as a catalyst. The solution was heated to 50°C in ten minutes, and remained at that temperature for 4 h with a stirring speed of 300 r/min until a pale yellow, viscous GU resin solution was acquired, then cooled to room temperature.

Treatment of specimens

All specimens were oven-dried at 103 ± 2°C and the initial oven-dried weights and sizes were measured before the impregnation. Different amount of nano-SiO_2 was dispersed in the synthesized GU resin by sonication for 30 minutes. The resin was impregnated into the specimens using a vacuum drying oven (0.1 bar, 30 min). After the impregnation, the excessive solution on the specimens was blotted off with a piece of tissue paper, and then placed the specimens in an oven for curing. The temperature was gradually increased to provide a curing temperature. The specimens were then cured for 4 h, finally oven-dried at 103°C to a constant weight. The final weights and sizes of the specimens were measured.

Physical properties

Weight percentage gain

Weight percentage gain (WPG) due to the chemical load was calculated as follows:

$$\mathrm{WPG}(\%) = [(\mathrm{Wt} - \mathrm{Wu})/\mathrm{Wu}] \times 100$$

where *Wu* and *Wt* are the oven-dried weights (g) of each wood sample before and after treatment, respectively.

Dimensional stability and water uptake

Poplar sapwood samples were cut and either treated or left untreated, then measured for dimensional stability and water absorption ability. Eight matched specimens for each group in 30 mm (tangential) × 30 mm (radial) × 10 mm (longitudinal) dimensions were prepared. The blocks were immersed in water for 24 h. After 24-h immersion their weights were measured after removing surface water with tissue paper, and the dimensions of the blocks were also measured using a digital micrometre (± 0.01 mm).

Based on the swelling difference between treated and control specimens, anti-swelling efficiency (ASE) was calculated as follows:

$$\mathrm{ASE}(\%) = [(\mathrm{Su} - \mathrm{St})/\mathrm{Su}] \times 100$$

where Su and St are the volumetric swelling of untreated and treated wood specimens, respectively.

As an index of water repellence efficiency from the initial and final weights after water saturation, water uptake (WU) of the specimens was calculated as follows:

$$\mathrm{WU}(\%) = [(\mathrm{Ww} - \mathrm{Wd})/\mathrm{Wd}] \times 100$$

where Ww and Wd are the weights of a specimens before and after the saturation with water, respectively.

Leaching test

After 24-h immersion, all specimens were oven-dried at 103 ± 2°C to a constant weight before measurement. Leachability (L) due to water immersion was calculated as follows:

$$\mathrm{L}(\%) = [(\mathrm{Wiw} - \mathrm{Wfw})/\mathrm{Wiw}] \times 100$$

where Wiw and Wfw are the dry weights of treated wood specimens before and after immersion, respectively.

Mechanical property testing

To evaluate the mechanical properties of treated and untreated wood, MOR, MOE, and CS were examined according to GB/T 1936.1-91 (*Method of testing in bending strength of wood*, China) and GB/T 1935-91 (*Method of testing in compressive strength parallel to grain of wood*, China) standards with a universal mechanical testing machine (MWW-50). Eight specimens were tested from each group.

Surface hardness (H) was measured by a TH 210 durometer (Beijing TIME High Technology Ltd., China) and expressed as shore D hardness according to the ASTM D2240 method. Twenty specimens were tested from each group.

Morphology characterization

The fracture morphology of treated and untreated wood after MOR and MOE testing was observed by camera. SEM was performed to characterize the distribution of GU resin and nano-SiO_2 on the wood cell walls. Tangential sections of treated and untreated wood specimens were mounted on conductive adhesives, sputter-coated with gold, and observed under SEM (Hitachi S-3400, Japan) at 15 KV voltages. In addition, the surface element contents of treated and untreated were also determined by EDX spectra.

Fourier transform infrared (FT-IR) spectroscopy

The treated and untreated wood specimens were ground to 160 mesh meal, embedded in potassium bromide (KBr) pellets, and examined by FT-IR (Nicolet 6700 Thermo Scientific, USA) in a scanning range of 4,000-400 cm^{-1} at 4 cm^{-1} resolution for 32 scans.

Thermal properties

Thermogravimetric analysis was conducted using a Q50 TGA analyser (TA Instruments, USA) at a heating rate of 10°C min^{-1} in a N_2 atmosphere from room temperature to 610°C. Roughly 3-5 mg of each sample was analysed.

Dynamic mechanical properties of the composites were measured using a dynamic mechanical analyser (Netzsch 242, Germany). Tests were performed using three-point bending model at oscillating amplitude of 60 μm and a frequency of 2 Hz. The temperature was swept from 40 to 230°C at a speed of 3°C min^{-1}. Each specimen dimension was 50 mm × 10 mm × 3 mm. Four replicates were conducted for each group.

Limiting oxygen index (LOI) test

LOIs of treated and untreated specimens were measured with a HC-2 oxygen index meter (Jiang Ning Analysis Instrument Company, China) with sheet dimensions (135 mm × 6.5 mm × 3 mm) according to ASTM D2863-77. Six replicates were tested from each group.

Acknowledgements

The authors are very grateful for financial support from Special Fund for Forestry Research in the Public Interest (Project 201204702) and the support from the China Scholarship Council (CSC).

Notes and references

1 C. M. Welch and G. F. Danna, *Text. Res. J.*, 1982, **52**, 149.
2 G. G. Xu, C. Q. Yang and Y. Deng, *J Appl Polym Sci*, 2002, **83**, 2539.
3 Z. Y. Yuan and H. R. Hu, *J Appl Polym Sci*, 2012, **126**, E459.
4 G. G. Xu, C. Q. Yang and Y. L. Deng, *J Appl Polym Sci*, 2004, **93**, 1673.
5 X. L. Cai, B. Riedl, S. Zhang and H. Wan, *Wood and Fiber Science*, 2007, **39**, 307.
6 S. Kittinaovarat, P. Kantuptim and T. Singhaboonponp, *J Appl Polym Sci*, 2006, **100**, 1372.
7 P. Navarrete, A. Pizzi, K. Rode, M. Vignali and H. Pasch, *J. Adhes. Sci. Technol.*, 2013, **27**, 586.
8 E. S. Lee and S. I. Kim, *J Appl Polym Sci*, 2005, **96**, 975.
9 C. M. Welch, *Text. Res. J.*, 1983, **53**, 181.
10 J. Weaver, J. Nielson and I. Goldstein, *Forest Products Journal*, 1960, **10**, 306.
11 T. Nakano, *Wood science and technology*, 1993, **28**, 23.
12 S. Yusuf, *Wood research: Bulletin of the Wood Research Institute Kyoto University*, 1996, **83**, 140.
13 R. Yasuda, K. Minato and M. Norimoto, *Wood Science and technology*, 1994, **28**, 209.
14 Y. T. Yan, Y. M. Dong, H. Chen, S. F. Zhang and J. Z. Li, *BioResources*, 2014, **9**, 4540.
15 J. Z. Li, T. Furuno, W. R. Zhou, Q. Ren, X. Z. Han and J. P. Zhao, *J Wood Chem Technol*, 2009, **29**, 241.
16 Y. J. Xie, A. Krause, H. Militz, H. Turkulin, K. Richter and C. Mai, *Holzforschung*, 2007, **61**, 43.
17 M. Deka and C. Saikia, *Bioresour Technol*, 2000, **73**, 179.
18 M. Deka, C. Saikia and K. Baruah, *Bioresour Technol*, 2002, **84**, 151.
19 W. Gindl, C. Hansmann, N. Gierlinger, M. Schwanninger, B. Hinterstoisser and G. Jeronimidis, *J Appl Polym Sci*, 2004, **93**, 1900.
20 T. Furuno, Y. Imamura and H. Kajita, *Wood Science and Technology*, 2004, **37**, 349.
21 C. P. Gabrielli and F. A. Kamke, *Wood science and technology*, 2010, **44**, 95.
22 X. D. Cao, Y. Habibi and L. A. Lucia, *Journal of Materials Chemistry*, 2009, **19**, 7137.
23 B. Jo, C. Kim, G. Tae and J. Park, *Constr Build Mater*, 2007, **21**, 1351.
24 H. J. Song, Z. Z. Zhang and X. H. Men, *Composites Part A*, 2008, **39**, 188.
25 A. Kinloch, R. Mohammed, A. Taylor, C. Eger, S. Sprenger and D. Egan, *J Mater Sci*, 2005, **40**, 5083.
26 Q. J. Lin, G. D. Yang, J. H. Liu and J. P. Rao, *Frontiers of Forestry in China*, 2006, **1**, 230.
27 H. N. Xu, S. F. Ma, W. P. Lv and Z. P. Wang, *Pigment & Resin Technology*, 2011, **40**, 191.
28 H. M. Lu, X. M. Xu, X. H. Li and Z. J. Zhang, *Bulletin of Materials Science*, 2006, **29**, 485.
29 W. J. Zou, J. Peng, Y. Yang, L. Q. Zhang, B. Liao and F. R. Xiao, *Materials Letters*, 2007, **61**, 725.
30 B. Blackman, A. Kinloch, J. S. Lee, A. Taylor, R. Agarwal, G. Schueneman and S. Sprenger, *J Mater Sci*, 2007, **42**, 7049.
31 J. S. Shi, J. Z. Li and W. R. Zhou, *China For Ind*, 2004, **7**, 48.
32 J. S. Shi, J. Z. Li, W. R. Zhou and D. R. Zhang, *Frontiers of Forestry in China*, 2007, **2**, 104.
33 R. R. Devi and T. K. Maji, *Wood Science and Technology*, 2012, **46**, 1151.
34 Y. M. Dong, Y. T. Yan, S. F. Zhang and J. Z. Li, *BioResources*, 2014, **9**, 6028.
35 N. Guigo, A. Mija, R. Zavaglia, L. Vincent and N. Sbirrazzuoli, *Polym Degrad Stab*, 2009, **94**, 908.
36 Y. T. Yan, Y. M. Dong, C. Li, H. Chen, S. F. Zhang and J. Z. Li, *Wood Science and Technology*, 2014, **49**, 241.
37 Y. J. Xie, Q. L. Fu, Q. W. Wang, Z. F. Xiao and H. Militz, *Eur J Wood Prod*, 2013, **71**, 401.
38 A. J. Crosby and J. Y. Lee, *Polym Rev*, 2007, **47**, 217.
39 S. D. Deng, X. H. Li, X. G. Xie and G. B. Du, *Chinese Journal of Structural Chemistry*, 2013, **32**, 1773.
40 W. Q. Song and C. J. Su, *East China Pulp & Paper Industry*, 2009, **40**, 65.
41 K. Harrington, H. Higgins and A. Michell, *Holzforschung-International Journal of the Biology, Chemistry, Physics and Technology of Wood*, 1964, **18**, 108.
42 A. Michell, A. Watson and H. Higgins, *Tappi*, 1965, **48**, 520.
43 Y. Sudiyani, Y. Imamura, S. Doi and S. Yamauchi, *Journal of wood science*, 2003, **49**, 86.
44 G. F. Wu, Q. Lang, H. Y. Chen and J. W. Pu, *BioResources*, 2012, **7**, 816.
45 M. S. Islam, S. Hamdan, Z. A. Talib, A. S. Ahmed and M. R. Rahman, *Compos Sci Technol*, 2012, **72**, 1995.
46 A. Hazarika, M. Mandal and T. K. Maji, *Composites Part B: Engineering*, 2014, **60**, 568.
47 A. Schniewind and J. Barrett, *Wood Science and Technology*, 1972, **6**, 43.
48 H. Gu, *Materials & Design*, 2009, **30**, 2774.
49 M. N. Xiong, G. X. Gu, B. You and L. M. Wu, *J Appl Polym Sci*, 2003, **90**, 1923.